RNA BIOLOGY
2019, VOL. 16, NO. 5, 626–638
https://doi.org/10.1080/15476286.2019.1572440

Taylor & Francis
Taylor & Francis Group

RESEARCH PAPER

Identification of a novel antisense RNA that regulates growth hormone receptor expression in chickens

Shudai Lin[a,b,c], Zihao Zhang[a], Tingting Xie[a], Bowen Hu[a], Zhuohao Ruan[a], Li Zhang[d], Congjun Li [b], Charles Li[c], Wen Luo[a], Qinghua Nie[a], and Xiquan Zhang[a]

[a]Guangdong Provincial Key Lab of Agro-Animal Genomics and Molecular Breeding and Key Lab of Chicken Genetics, Breeding and Reproduction, Ministry of Agriculture, College of Animal Science of South China Agricultural University, Guangzhou, P.R. China; [b]Animal Genomics and Improvement Laboratory, Agricultural Research Service, United States Department of Agriculture, Beltsville, MD, USA; [c]Animal Biosciences and Biotechnology Laboratory, Agricultural Research Service, United States Department of Agriculture, Beltsville, MD, USA; [d]Agricultural College, Guangdong Ocean University, Zhanjiang, P.R. China

ABSTRACT

Natural antisense transcripts (NATs) are widely present in mammalian genomes and act as pivotal regulator molecules of gene expression. However, studies on NATs in the chicken are relatively rare. We identified a novel antisense transcript in the chicken, designated *GHR-AS-EST*, transcribed from the growth hormone receptor (*GHR*) locus, which encodes a well-known regulatory molecule of muscle development and fat deposition. *GHR-AS-EST* is predominantly expressed in the chicken liver and muscle tissues. *GHR-AS-EST* sequence conservation among vertebrates is weak. *GHR-AS-EST* forms an RNA–RNA duplex with *GHBP* to increase its stability, and regulates the expression of *GHR* sense transcripts at both the mRNA and protein levels. Further, *GHR-AS-EST* promotes cell proliferation by stimulating the expression of signaling factors in the JAK2/STAT pathway, and contributes to fat deposition via downregulating the expression of signaling factors in the JAK2/SOCS pathway in LMH hepatocellular carcinoma cells. We expect that the discovery of a NAT for a regulatory gene associated with cell proliferation and lipolysis will further our understanding of the molecular regulation of both muscle development and fat deposition.

ARTICLE HISTORY
Received 26 November 2018
Revised 6 January 2019
Accepted 17 January 2019

KEYWORDS
Natural antisense transcript; chicken; GHR; GHBP; RNA–RNA duplex; fat deposition

Introduction

Antisense RNAs, also called natural antisense transcripts (NATs), are transcribed from the DNA strand opposite to the strand of their specific protein-coding or noncoding gene and overlap with the sense transcript [1,2]. Some NATs can form double-stranded RNAs with other transcripts according to the base complementary rule. Based on whether they work on *cis* or *trans*, NATs are grouped into cis-NATs and trans-NATs [3]. NATs belong to the family of long non-coding RNAs (lncRNAs) and have been divided into head-to-head, tail-to-tail, and fully overlapped categories in reference to their sense transcripts [4–8]. Various techniques and methods have been applied to identify NATs and to characterize their functions based on transcriptome data [3,9,10], chromatin features, genome distribution, expression pattern, and subcellular localization [6,11]. NATs regulate target genes expression at several levels, including transcription, mRNA processing, splicing, RNA stability, cellular transport and translational regulation [3,12,13]. Both sense and antisense RNAs can encode proteins or be non-protein -coding transcripts [2]. However, the functions of NATs are mostly unknown. Identifying functional coding or non-coding antisense RNAs and inferring biological pathways in which they act represent major challenges in understanding genome complexity and RNA-mediated gene regulation.

The actions of growth hormone (GH) are mediated via the growth hormone receptor (GHR) [14]. Both human Laron-type dwarfism and sex-linked dwarfism in the chicken are caused by *GHR* mutation [15–17]. Chicken *GHR* produces several sense transcripts through alternative usage of different 5′ untranslated regions (UTRs) and a functional polyadenylation signal [16,18–20] (Fig. S1). *GHR* mRNA encodes a full-length GHR protein that contains an extracellular domain, a transmembrane domain, and an intercellular domain [21], a truncated GH-binding protein (GHBP), that comprises only the extracellular hormone-binding domain of GHR [20], and a truncated 0.7-kb transcript that might encode a 27.5-kDa protein [18]. GHBP can recognize and bind to GH, which reduces the amount of GH bound to GHR [20]. In the liver, GH and GHR together with insulin-like growth factor (IGF) form the GH-GHR-IGF signal pathway that regulates various physiological processes, including cell proliferation and differentiation, as well as sugar, protein, fat metabolism, through promoting the transcription of related genes, such as insulin receptor substrate (*IRS*), cytokine signaling 3 (*SOCS3*), and leptin receptor (*LEPR*), which ultimately determine animal growth and development [15,16,22].

NATs have been reported for numerous genes [7,23]. In our previous study, we identified NATs originating from more than 7,200 genes that were extensively expressed in the chicken liver by

CONTACT Xiquan Zhang xqzhang@scau.edu.cn Guangdong Provincial Key Lab of Agro-Animal Genomics and Molecular Breeding and Key Lab of Chicken Genetics, Breeding and Reproduction, Ministry of Agriculture, College of Animal Science of South China Agricultural University, Guangzhou 510642, P.R. China

This article has been republished with minor change. This change do not impact the academic content of the article.

using digital gene expression sequencing of RNA [24]. In addition to known expressed NATs, a 4,337 nucleotide (nt)-long NAT transcribed from the opposite strand of the *GHR* 3′UTR to intron 6 (Fig. S1B), which we termed *GHR-AS* [16]. In this study, we identified and characterized a novel intronic NAT of *GHR* transcribed from the opposite strand of *GHR* gene intron 5 to the 5′UTR, termed *GHR-AS-EST*. It highly expresses in normal chicken liver and leg muscle tissues. *GHR-AS-EST* suppresses *GHR* mRNA expression by repressing the transcriptional activity of the *GHR* V1 promoter. Surprisingly, the expression of *GHBP* and 0.7-kb *GHR* was stimulated when the transcriptional activity of the V1 promoter was reduced. We report that *GHR-AS-EST* does not stabilize *GHR* mRNA and the 0.7-kb transcript, but it does stabilize *GHBP* by forming an RNA–RNA duplex *in vitro* and *in vivo*, and that it decreases GHR expression, but increases the expression of GHBP and the 0.7-kb transcript at both the RNA and the protein level. *GHR-AS-EST* contributes to cell proliferation and fat deposition in LMH hepatocellular carcinoma cells by binding GHBP to influence GH-GHR signaling, promoting JAK2/STAT and suppressing JAK2/SOCS signaling. Moreover, the chicken *GHR-AS-EST* sequence shows weak similarity with those of other vertebrates, suggesting that it might be a species-specific NAT.

Results

GHR-AS-EST is strongly expressed in chicken liver and muscle tissues

From the expressed sequence tag (EST) sequences in the NCBI UniGene database (http://www.ncbi.nlm.nih.gov/UniGene), BX263735.2 was identified as a NAT that is transcribed from the negative strand of the Gallus gallus *GHR* locus and comprises more than three exons of the *GHR* gene (exons 1, 2, 4 and a portion of exon 5). To confirm that BX263735.2 originates from the reverse strand of the *GHR* locus, we conducted strand-specific reverse transcription (RT-)PCR, rapid amplification of cDNA ends (RACE) and northern blot analyses of White Recessive Rock (WRR) chicken liver tissues. As shown in Figs. S2 and S3, BX263735.2 was successfully amplified (Fig. S3A–C), and its entire sequence (688 bp with GC-rich in 3'UTR) matched the sequence 'CATGGATCCCAGTTTGACTAG' sequence (Fig. S3D), which was previouly identified from the *GHR* negative strand at exon 6 [24]. These findings confirmed that BX263735.2 is a novel NAT of the *GHR* locus in the chicken genome. Moreover, this NAT was complementary to *GHR* pre-mRNA from the 5′UTR to exon 6. Therefore, we referred to BX263735.2 as the *GHR* antisense EST (*GHR-AS-EST*) transcript. *GHR-AS-EST* was classified as an antisense lncRNA based on its low coding potential as calculated using Coding Potential Calculator (CPC) software [25,26] (Fig. S3E). However, based on analysis of LMH cells transfected with pCMV-GHR-AS-EST-C-Flag vector, the transcript might encode a 17-kDa protein (Figure 1A). The transcript is expressed in both cytoplasmic and nuclear fractions of chicken primary myoblasts (Figure 1B). Next, we quantified *GHR-AS-EST* expression by RT-qPCR in 13 tissues from six 16-day-old WRR chicken embryos. *GHR-AS-EST* expression was the highest in the heart, followed by the liver, glandular stomach, and leg muscle, and it was the lowest in gizzard tissue (Figure 1C).

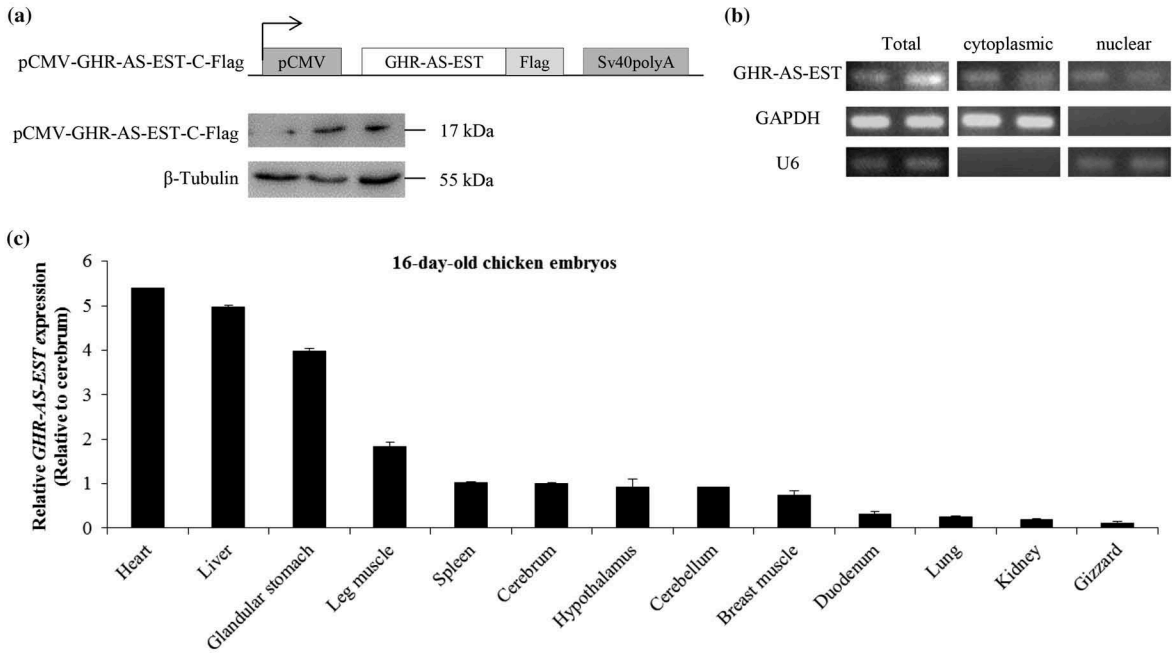

Figure 1. Chicken *GHR-AS-EST* does encode a protein.

(A) Western blot analysis of the coding ability of *GHR-AS-EST*. The upper panel shows a schematic representation of pCMV-GHR-AS-EST-C-Flag vector. The whole sequence of *GHR-AS-EST* was cloned into the eukaryotic expression vector, pCMV-C-Flag. The lower panel showed the western blot results. LMH cells transfected with β-tubulin were used as a positive control (N = 3). (B) RT-qPCR detection of *GHR-AS-EST* in cytoplasmic and nuclear fractions of chicken primary myoblasts. *GAPDH* and *U6* serve as cytoplasmic and nuclear localization controls, respectively. (C) *GHR-AS-EST* expression profile in WRR chicken tissues. Data are representative of three independent assays using tissues from six female 16-day-old WRR chickens embryos and shown as the mean ± SEM.

GHR-AS-EST suppresses GHR mRNA expression, but promotes the expression of both GHBP and 0.7-kb GHR

The V1 GHR sense promoter reportedly drives the transcription of GHR sense transcript [27]. In this study, we identified an antisense promoter (ASP) of *GHR* located in intron 5 and 99 bp away from the 5′ end of *GHR-AS-EST*, which drives the expression of *GHR-AS-EST* (Figures 2A and S4). Given the reports on NAT regulation of host gene expression [16,28–30], and the potential overlap region between the *GHR* sense transcripts and *GHR-AS-EST* (Figure 2A), we predicted that the overlap between *GHR-AS-EST* and *GHR* was indicative of an underlying regulatory effect. To confirm this, we constructed an interfering oligo (si-GHR-AS-EST) and a GHR-AS-EST overexpression vector (pc3.1-GHR-AS-EST), and transfected them into LMH cells. After 48 h, the relative mRNA levels of *GHR* and *IGF1* were significantly enhanced after GHR-AS-EST knockdown ($p < 0.05$) and supressed by >55% following GHR-AS-EST overexpression ($p < 0.01$) when compared to levels in the respective control cells, as indicated by RT-qPCR (Figure 2B and E). In contrast, the relative RNA levels of *GHBP* and *0.7-kb GHR* were significantly lower after GHR-AS-EST knockdown ($p < 0.05$) and significantly higher after GHR-AS-EST overexpression than in the respective control cells (Figure 2C and D)). Protein expression levels of GHR, GHBP, and 0.7-kb GHR were consistent with the RNA levels (Figure 2F–H). These results indicated that GHR-AS-EST suppresses *GHR* mRNA and protein expression, but promotes RNA and protein expression of GHBP and 0.7-kb GHR.

GHR-AS-EST inhibits GHR mRNA expression by suppressing the transcriptional activity of the V1 sense promoter

To evaluate the regulatory functions of GHR-AS-EST in the expression of the various GHR transcripts, we examined the transcriptional activity of the *GHR* V1 promoter in LMH

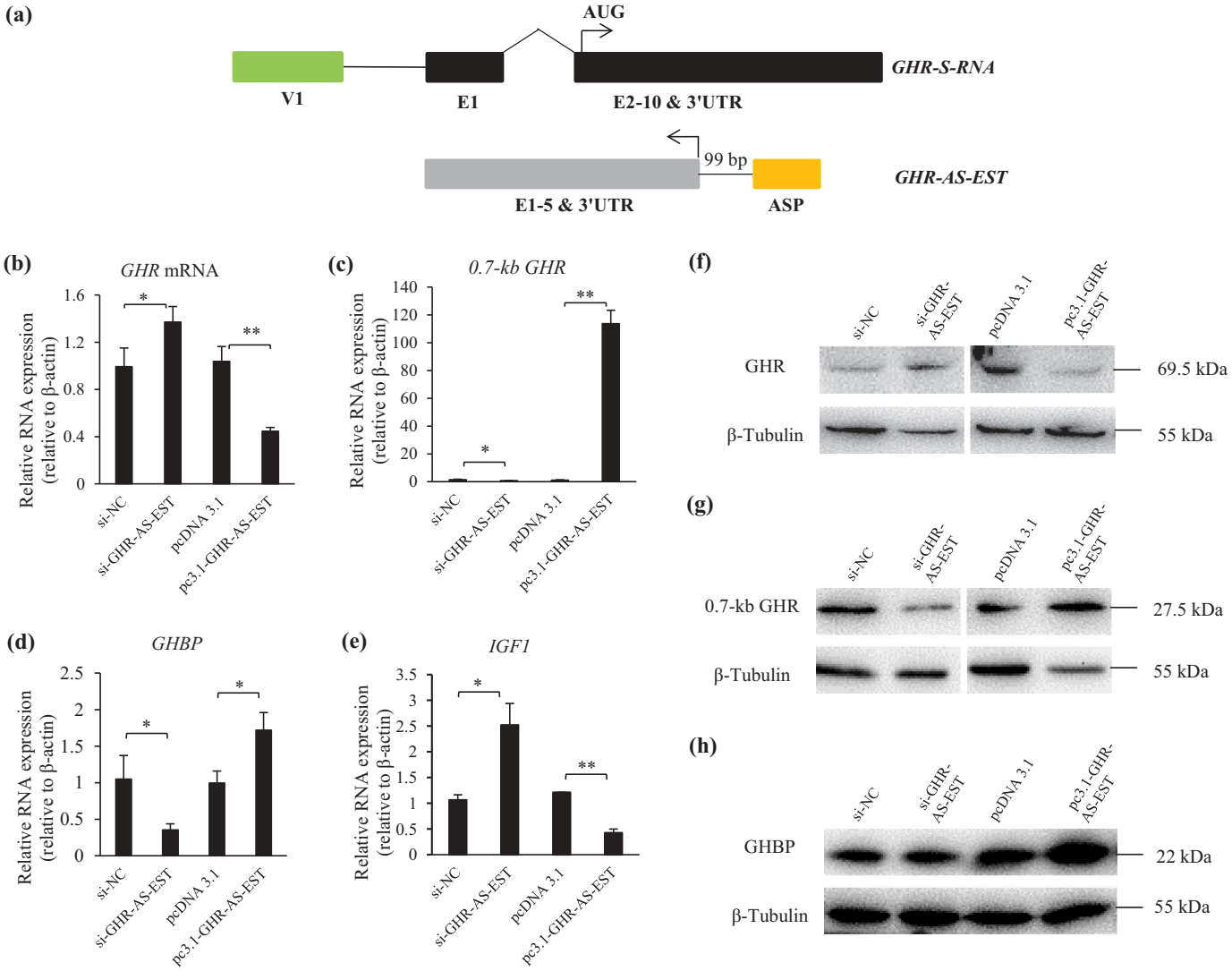

Figure 2. *GHR-AS-EST* inhibits GHR expression, but promotes the expression of 0.7-kb GHR and GHBP.

(A) Schematic representation of the structure and transcriptional orientation of *GHR* sense transcript (*GHR-S-RNA*) or antisense RNA (*GHR-AS-EST*). Green and orange boxes: *GHR* sense promoter V1 and antisense promoter (ASP), respectively. E: exon. UTR: untranslated region. AUG in *GHR-S-RNA* represents the translation initiation codon. The 5′ end of *GHR-AS-EST* is 99 bp away from ASP. Relative RNA expression levels of *GHR* mRNA (B), *0.7-kb GHR* (C), *IGF1* (D) and *GHBP* (E) in treated LMH cells. Data are the mean ± SEM and are representative of triplicate experiments. Protein expression levels of GHR (F), 0.7-kb GHR (G), and GHBP (H) in treated LMH cells. *$p < 0.05$; **$p < 0.01$.

cells. A pEGFP reporter gene assay revealed that the transcriptional activity of *GHR* V1 was significantly increased after treatment of LMH cells with si-GHR-AS-EST when compared with the control (si-NC) ($p < 0.05$) (Fig. S5A). Opposite findings were obtained in an overexpression assay ($p< 0.05$) (Fig. S5B). A pGL3-basic promoter reporter assay revealed similar results: *GHR* V1 transcriptional activity was enhanced by 39% in GHR-AS-EST knockdown LMH cells as compared to control cells ($p < 0.05$), and was suppressed by 38% in GHR-AS-EST-overexpressing LMH cells as compared to control cells ($p < 0.01$) (Figure 3). Together, these results demonstrated that GHR-AS-EST suppresses *GHR* V1 transcriptional activity, thus affecting *GHR* mRNA expression. Unexpectedly, *GHBP* and *0.7-kb GHR* expressions were increased when *GHR* V1 transcriptional activity was decreased. Based on these results, we hypothesized that *GHR-AS-EST* downregulates the transcriptional activity of *GHR* V1 to inhibit *GHR* mRNA expression, whereas expression of *GHBP* and *0.7-kb GHR* is upregulated through another mechanism.

GHR-AS-EST upregulates GHBP expression by forming an RNA duplex in vivo and in vitro

Antisense RNAs reportedly form duplexes with their sense mRNA partners [12,13,16,31,32], and these duplexes regulate the stability of the coding mRNA and thus, the protein level [2,33]. To determine whether *GHR-AS-EST* forms a duplex with *GHR* sense transcripts, including *GHR* mRNA, *GHBP* and *0.7-kb GHR*, we carrried out an endogenous RNase protection assay using RNA extracted from liver and leg muscle tissues, LMH cells, and primary myoblasts. Only the overlapping region at exons 2-6 of *GHR* mRNA was retained (Figure 4A and B)), indicating that *GHR-AS-EST* and *GHR* sense transcript form a 537-bp RNA duplex *in vivo* and *in vitro*. Next, we conducted an mRNA stability assay to investigate whether GHR-AS-EST overexpression would enhance *GHR* sense transcripts stability. Compared to cells transfected with an empty vector (pcDNA 3.1), GHR-AS-EST-overexpressing (pc3.1-GHR-AS-EST) cells demonstrated increased stability of *GHBP*, but not *GHR* mRNA and *0.7-kb GHR* (Figure 4C), which was consistent with the results on the protein levels of both GHBP and GHR (Figure 2F and H). These findings suggested that *GHR-AS-EST* enhances the stability of *GHBP* RNA by forming a duplex, and thus regulate its protein level.

Localization of GH and GH dimerization with different GHR proteins in living cells

To directly investigate the localization and dimerization of GH and/or different GHR proteins in living cells, we conducted fluorescence colocalization assay by transfecting LMH cells with GH_{CFP}, GHR_{EGFP}, $GHBP_{YFP}$, 0.7-kb $GHR_{BFP,}$ or GHR-AS-EST_{DsRed} (Fig. S6A-B), or GH_{YFP}/$GHBP_{DsRed}$, 0.7-kb GHR_{YFP} /GHR-AS-EST_{DsRed}, GH_{YFP}/0.7-kb GHR_{DsRed}, or GH_{YFP}/GHR-AS-EST_{DsRed} (Fig. S6C). Strikingly, GH, GHR and GHBP were expressed only in the cytosol (Fig. S3B and D(a)), whereas 0.7-kb GHR and GHR-AS-EST were expressed in both the cytosol and the nucleus (Fig. S6D(c), (d)). Fluorescence resonance energy transfer (FRET) was used to visually monitor the dimerization of the six above pairs in living LMH cells. We first optimized the filter settings to make sure no crossover excitation of blue fluorescent protein (BFP) occurred when DsRed was excited. For this purpose, we individually transfected GH_{BFP}, $GHBP_{BFP}$, GHR-AS-EST_{BFP}, $GHBP_{DsRed}$, 0.7-kb GHR_{DsRed}, or GHR-AS-EST_{DsRed} into chicken primary myoblasts cells. Cells transfected with GH_{BFP}, $GHBP_{BFP}$ or GHR_{BFP} alone exhibited blue fluorescence under excitation at 382 nm and emission at 435–465 nm, and no fluorescence signal was detected in the bandwidth of 570–600 nm ($GHBP_{DsRed}$, 0.7-kb GHR_{DsRed}, GHR-AS-EST_{DsRed} channel) (Figure 5A–F, upper panels). Similarly, cells transfected $GHBP_{DsRed}$, 0.7-kb GHR_{DsRed}, or GHR-AS-EST_{DsRed} alone exhibited red fluorescence under excitation at 558 nm and emission at 570–600 nm, without crossover to the BFP channel (emission at 435–465 nm) (Figure 5A–F, middle panels). At the optimal FRET setting,

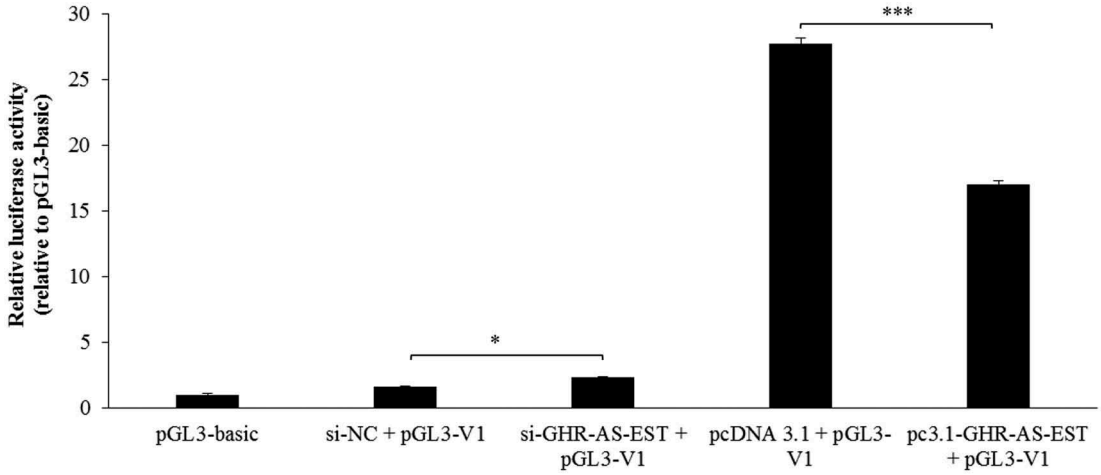

Figure 3. *GHR-AS-EST* decreases the transcriptional activity of the *GHR* V1 promoter.

Relative transcriptional activity changes of the *GHR* V1 promoter after knockdown and overexpression of *GHR-AS-EST*. Data are shown as fold induction compared with the activity of LMH cells transfected with pGL3-basic (promoter-less) luciferase reporter vector, and are the mean ± SEM of at least three experiments. *$p < 0.05$; ***$p < 0.001$.

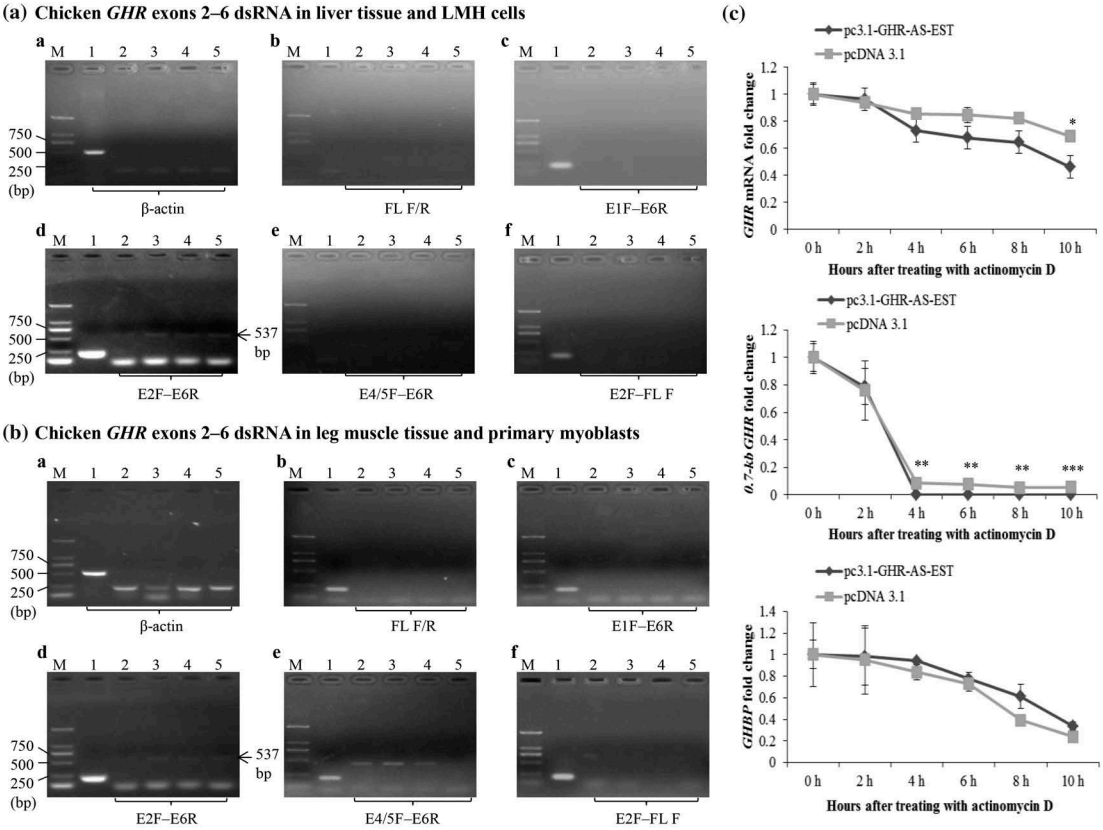

Figure 4. *GHR-AS-EST* upregulates *GHBP* expression by forming an RNA duplex in exons 2–6.

(A) Chicken *GHR* exons 2–6 RNA duplex detected in liver tissue and LMH cells. (B) Chicken *GHR* exons 2–6 RNA duplex detected in leg muscle tissue and primary myoblasts. (a) lane 1: DNA template as a positive control; lanes 2 and 3, the template is cDNA that is strand-specifically reverse-transcribed from 12-day-old WRR chicken embryo liver tissues (A) or leg muscle tissue (B); lanes 4 and 5, the template is cDNA that is strand-specifically reverse-transcribed from LMH cells (A) or primary myoblasts (B). (**b–**f) lane 1: cDNA is the template as a positive control; lanes 2–5, the templates are the same as those in panel (a). Marker (M): 2000, 1200, 750, 500, 250, and 100 bp. The black triangle indicated the RNA duplex formed by *GHR-S* and *GHR-AS-EST* with a total length of 537 bp. (C) mRNA stability assay results. Data are shown as the mean ± SEM of at least three experiments. *$p < 0.05$; **$p < 0.01$; ***$p < 0.001$.

excitation of GH_{BFP}, $GHBP_{BFP}$, or GHR-AS-EST_{BFP} (donor) at 382 nm produced a diffuse image of $GHBP_{DsRed}$, 0.7-kb GHR_{DsRed}, or GHR-AS-EST_{DsRed} (acceptor) at 570–600 nm (Figure 5A–F), bottom panels), suggesting that FRET occurred from GH_{BFP} to $GHBP_{DsRed}$, 0.7-kb GHR_{DsRed}, or GHR-AS-EST_{DsRed}, $GHBP_{BFP}$ to 0.7-kb GHR_{DsRed} or GHR-AS-EST_{DsRed}, and GHR-AS-EST_{BFP} to 0.7-kb GHR_{DsRed}.

GHR-AS-EST blocks signal transmission from GH to GHR and from GHR to STAT5 by promoting GHBP expression

For signaling, GH needs to bind to a GHR dimer, which modifies the position of the GHR extracellular domains and activates JAK2-STAT signaling [17,34]. GHBP inhibits the binding of GH to GHR by forming a GH–GHBP complex [20]. Though GHBP and 0.7-kb GHR expression was upregulated by GHR-AS-EST (Figure 2), whether 0.7-kb GHR regulated *GHR* mRNA and *GHR-AS-EST* expression remained unknown. In LMH cells transfected with pc3.1-0.7-kb GHR overexpression plasmid, unexpectedly, *GHR* mRNA expression was not affected, whereas *GHR-AS-EST* expression was significantly enhanced ($p < 0.01$) (Fig. S7A). However, in LMH cells cotransfected with pc3.1-0.7 kb GHR and pc3.1-GHR-AS-EST, *GHR* mRNA expression was suppressed ($p < 0.05$) (Fig. S7B). We hypothesized that GHR-AS-EST can be induced by 0.7-kb GHR and affect the signal transduction from GHR to STAT5 by influencing GHBP expression. To confirm this hypothesis, we explored the RNA level of different factors involved in JAK2/STAT and JAK2/MAPK signaling (Figure 6A). Upon GHR-AS-EST knockdown, *GH* mRNA expression was increased, whereas the relative expression of *STAT1-6*, RAS guanyl releasing protein (*RASGRP*), B-Raf proto-oncogene (*BRAF*), Raf-1 proto-oncogene (*RAF1*), and mitogen-activated protein kinase kinase 2 (*MAP2K2*) was decreased (Figure 6B and D). In contrast, *JAK2, STAT1, STAT2, STAT6* and *MAP2K2* expression was appreciably enhanced after GHR-AS-EST overexpression (Figure 6C and E). Cell proliferation was strongly stimulated in expression LMH cells overexpressing GHR-AS-EST, as indicated by cell-cycle analysis, CCK8 and EdU assays (Figure 6F–K).

GHR-AS-EST stimulates fat deposition via JAK2/SOCS signaling

SOCS3 induces fat deposition by suppressing *IRS1, LEPR* and *JAK* expression. Additionally, the *GHR* gene regulates SOCS3 through JAK/STAT signaling [15,22]. This suggests that GHR plays a role in fat deposition. Hence, we deduced that *GHR-AS-ETS* might regulate fat deposition, too. To verify this, we evaluated the RNA levels of different factors involved in JAK2/SOCS signaling (Figure 7A). *SOCS3, IRS1*, and *LEPR* mRNA levels

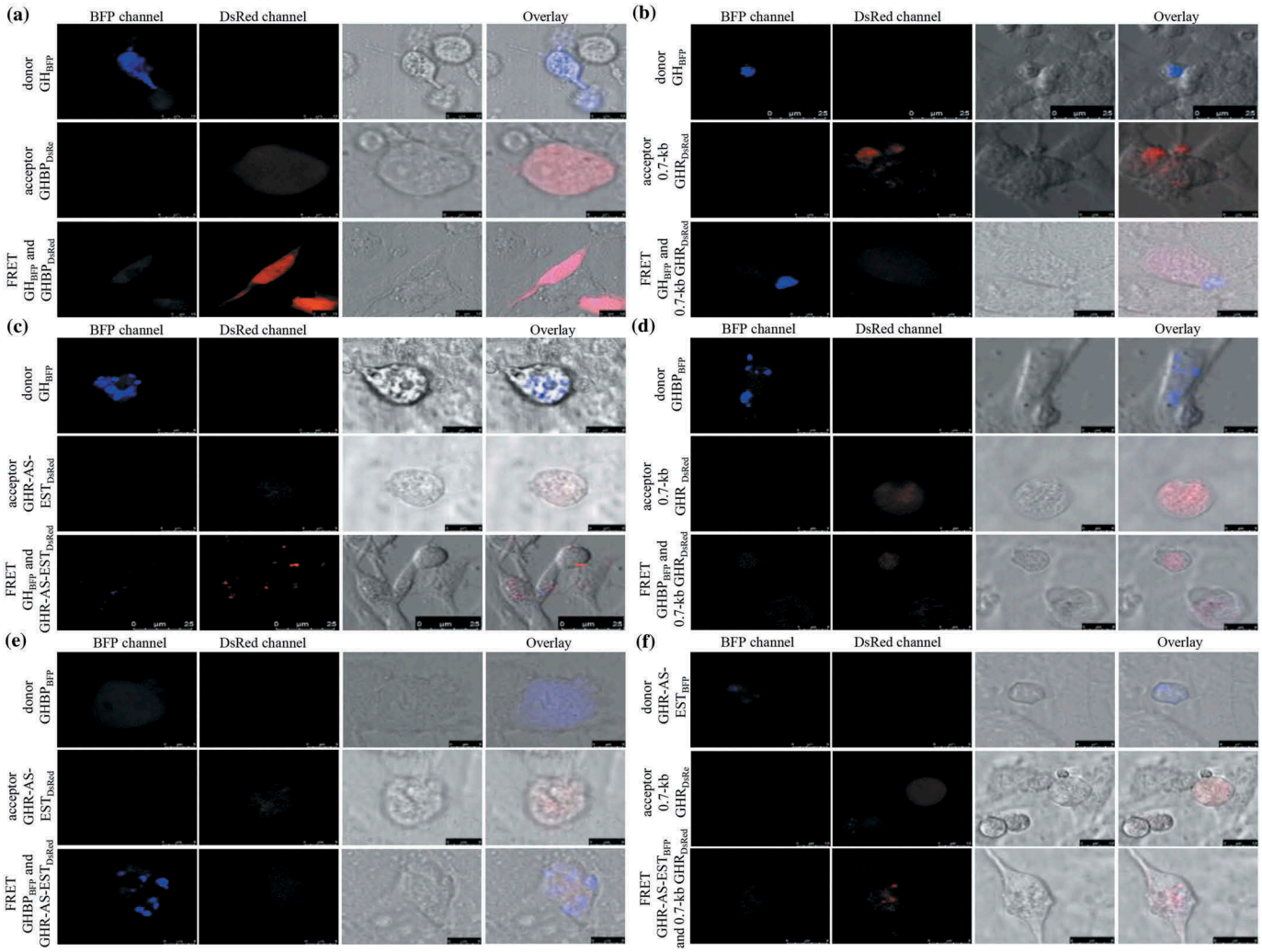

Figure 5. FRET analysis.

Chicken primary myoblasts were transfected with GH_{BFP}, $GHBP_{BFP}$, GHR-AS-EST_{BFP}, $GHBP_{DsRed}$, 0.7-kb GHR_{DsRed}, or GHR-AS-EST_{DsRed}, and 48 h later, the cells were observed under a confocal microscope with optimal filter sets. Cells containing GH_{BFP}, $GHBP_{BFP}$ and GHR-AS-EST_{BFP} were observed and imaged with excitation of BFP (A–F, upper left panels), with no crossover with the DsRed channel (A–F, upper second panels). Conversely, in cells containing $GHBP_{DsRed}$, 0.7-kb GHR_{DsRed} and GHR-AS-EST_{DsRed}, DsRed was excited and imaged in the DsRed channel only (A–F, middle left panels) without crossover with the BFP channel (A–F, middle second panels). Cells containing both GH_{BFP} and $GHBP_{DsRed}$, GH_{BFP} and 0.7-kb GHR_{DsRed}, GH_{BFP} and GHR-AS-EST_{DsRed}, $GHBP_{BFP}$ and 0.7-kb GHR_{DsRed}, $GHBP_{BFP}$ and GHR-AS-EST_{DsRed}, or GHR-AS-EST_{BFP} and 0.7-kb GHR_{DsRed} were observed at the excitation of the donor (BFP) and collection of both donor (BFP) (A–F, bottom left panels) and acceptor (DsRed) emission (A–F, bottom second panels) using optimal FRET settings. Corresponding phase-contrast and overlay images of the cells are presented in (A–F, third panels) and (A–F, right panels), respectively.

were appreciably suppressed after GHR-AS-EST overexpression as indicated by RT-qPCR ($p < 0.01$; Figure 7B–D). In contrast, mRNA expression of *SOCS3* and *LEPR* was significantly enhanced after *GHR-AS-EST* knockdown ($p < 0.05$ and $p < 0.01$, respectively, Figure 7B–D). Oil Red O staining assay indicated that fat deposition in LMH cells was lowered upon *GHR-AS-EST* knockdown, but enhanced by *GHR-AS-EST* overexpression (Figure 7E and F). These findings showed that chicken *GHR-AS-EST* can facilitate fat deposition, and we suggest via either inhibition of signal transduction from GH to GHR and from GHR to SOCS3 via a decrease in *GHR* mRNA expression and an increase in *GHBP* expression; or through direct inhibition of signal transduction in JAK2/SOCS pathway. Unexpectedly, although chicken GHR-AS-EST contains the sequence that is complementary to the exons 2-6-coding region of GHR, it exhibites <60% sequence identity with sequences of other species, as indicated by MEGA6.0 analysis (Table 1), BLAST2P with E-value >0.001, and other methods (data not shown), indicating low sequence conservation.

Discussion

NATs can originate from an intron of the host gene [5,35]. Here, we report *GHR-AS-EST*, a 688-bp and GC-rich RNA transcribed in antisense direction from intron 5 of the *GHR* gene. *GHR-AS-EST* represses *GHR* expression and promotes *GHBP* and *0.7-kb GHR* expression. This finding indicated that the antisense RNA could divergently regulate host gene expression. NATs having an inverse relationship with host genes have been reported in numerous studies. For example, *p15AS* could silence *p15* in *cis* and in *trans* through heterochromatin formation [29]; the NAT of Apolipoprotein A1 (*APOA1-AS*) was shown to repress *APOA1* expression in humans and monkeys [36]; nucleolar protein 14-*AS1* anti-correlates with its sense

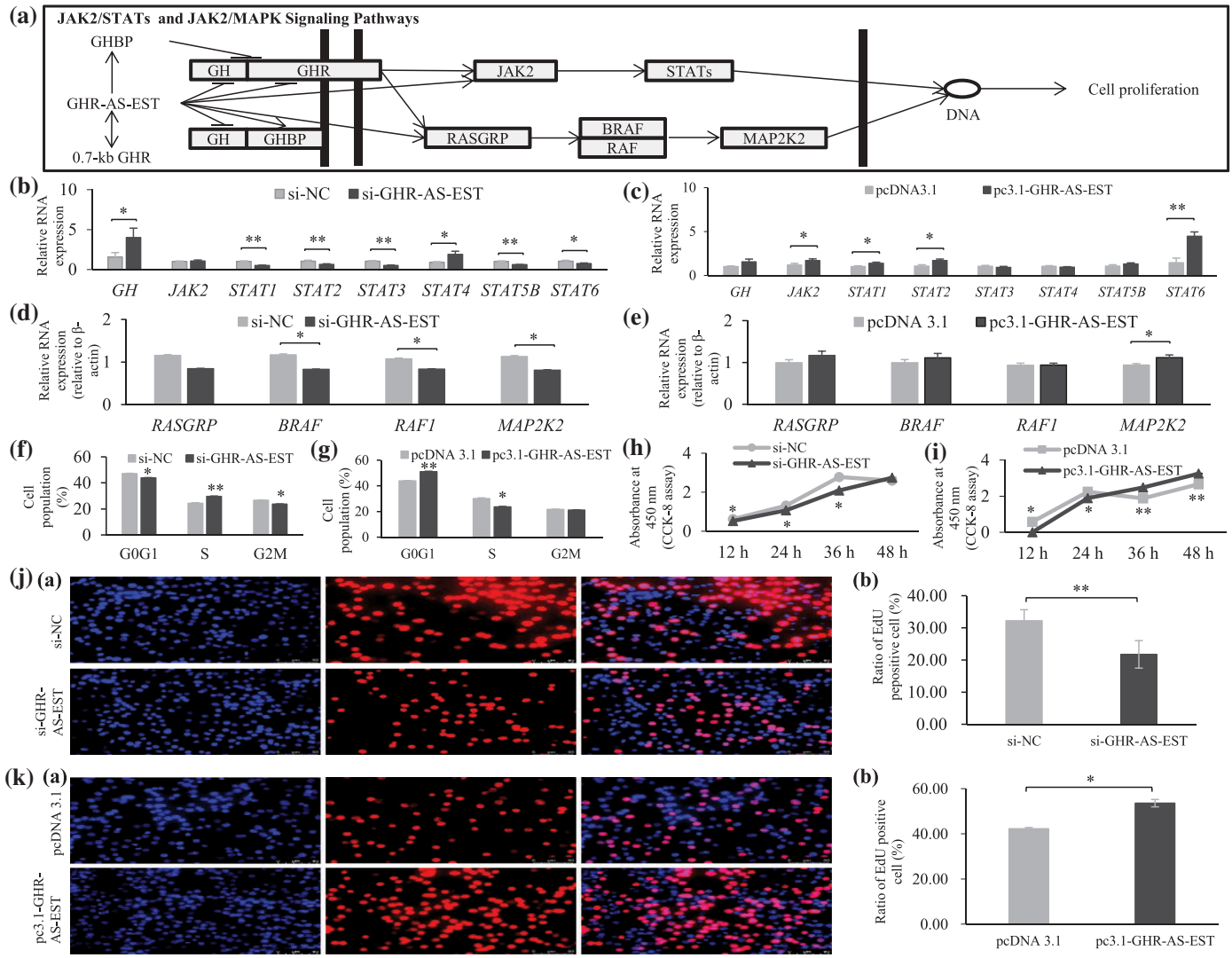

Figure 6. *GHR-AS-EST* positively regulates JAK2/STAT and JAK2/MAPK signaling.

(A) Schematic diagram of the JAK2/STAT and JAK2/MAPK signaling pathways. (B–E) Relative expression levels of *GH, JAK2, STAT1-6*, and *MAP2K2* in treated LMH cells. (F) and (G) Cell cycle analysis of treated LMH cells. (H) and (I) CCK8 assay results. (J) and (K) Proliferating cell fractions (%) in treated LMH cells (magnification, 400×). Data are the mean ± SEM of at least three experiments. *$p < 0.05$; **$p < 0.01$.

gene [37]; and a NAT of low-density lipoprotein receptor-related protein 1 downregulates the latter's expression [38]. However, some sense/antisense transcript pairs are concordantly expressed in a cell type or a tissue. For example, *Sirtuin 1* is concordantly expressed with its antisense partner during myogenic differentiation of mouse C2C12 cells [25]. Additionally, a NAT as well as a short splice variant of PTEN induced putative kinase 1 coexist in human neuroblastoma cells and human skeletal muscle tissue [39].

RNA duplex formation may mask pivotal regulatory features within transcripts to restrain the binding of other trans-acting factors. RNA masking intervenes with mRNA splicing, transport, polyadenylation, translation, and degradation [4,40]. Some NATs pair with their host genes to regulate epigenetic silencing, transcription and mRNA stability [12]. Increasing numbers of functional NATs are being identified in animals, such as mice, pigs, sheep, and chickens. For example, a NAT targeting the mouse gene encoding ubiquitin carboxy-terminal hydrolase L1 which is involved in brain function and neurodegenerative diseases, has been showed to regulate the synthesis of corresponding protein at the post-transcriptional level [12]. A phospholipase A2 group XVI locus (*PLA2G16*) NAT transcribed from porcine *PLA2G16* promotes *PLA2G16* transcription and might stimulate adipogenesis in pigs [31]. We previously identified a *GHR-AS* that enhanced *GHR* mRNA stability by forming an RNA–RNA duplex at the last exon of *GHR* mRNA in chicken LMH cells [16]. In this study, we uncovered a novel antisense RNA of chicken *GHR, GHR-AS-EST*, which decreases *GHR* mRNA and *0.7-kb GHR* stability but increases *GHBP* stability by forming an RNA–RNA duplex at the exons 2-6 of the *GHR* sense transcripts, as shown by *in-vivo* and *in-vitro* experiments. Exon 2 of *GHR* mRNA is necessary for GHR translation because it possesses the translation initiation codon (AUG) [20,41]. Exons 2-6 are required for GH–GHR binding [42,43]. GHBP prolongs the half-life of GH by forming a GHBP–GH complex. However, this complex formation inhibits GH–GHR binding [20]. Hence, hybridization of *GHR-AS-EST* to exons 2-6 of GHBP might supresses GH–GHBP binding and thus increase the probability for GH to bind with the GHR.

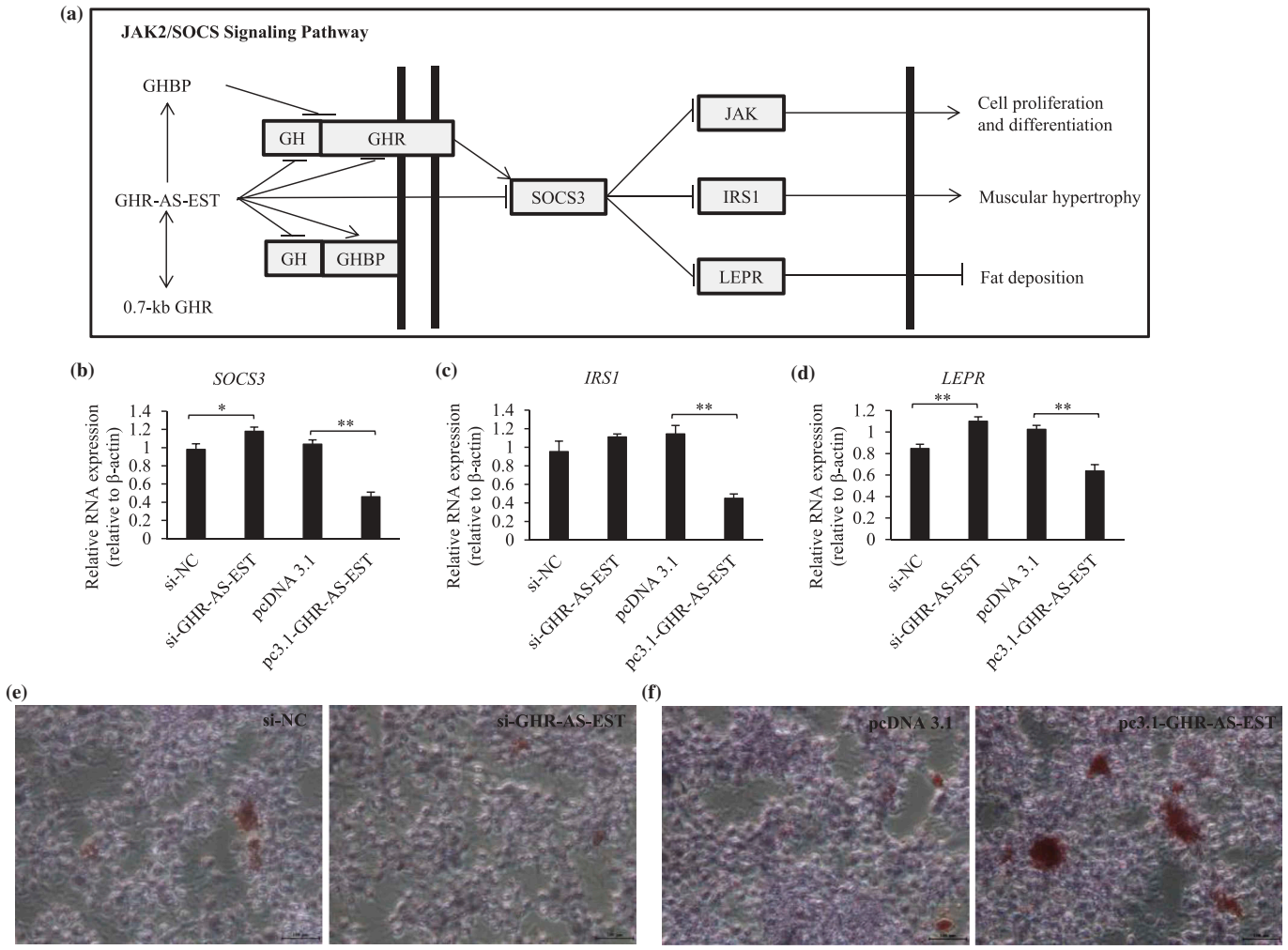

Figure 7. *GHR-AS-EST* increase fat deposition in LMH cells.

(A) Schematic diagram of JAK2/STAT and signaling pathway. (B–D) Relative expression levels of *SOCS3*, *IRS1*, and *LEPR* in treated LMH cells. Data are the mean ± SEM of at least three experiments. (E) and (F) Oil Red O staining analysis of fat deposition in treated LMH cells (magnification, 40×). *$p < 0.05$; **$p < 0.01$.

Table 1. Pair distances of *GHR-AS-EST* among different species.

					Divergence							
Sheep	Norway rat	Pig AJ94061	Pig AJ687535	BY775223.1	BU757735.1	Human	frog	medaka	Dog	Cattle	Chicken	Pencent identity
350.0	40.5	191.0	148.9	350.0	109.1	350.0	151.2	277.3	41.4	190.5		Chiken
350.0	191.7	12.8	221.3	231.4	178.5	221.1	98.6	186.5	193.2		2.9	Cattle
350.0	23.8	212.4	157.3	350.0	119.3	350.0	181.5	224.8		4.1	59.9	Dog
350.0	186.4	171.5	350.0	350.0	180.3	99.5	150.4		11.5	3.7	4.5	Japaness medaka
350.0	181.5	97.9	192.1	297.3	242.4	218.9		2.8	2.8	14.4	5.7	African clawed frog
221.3	350.0	224.7	350.0	170.1	230.8		4.8	6.0	2.8	5.3	14.3	Human
350.0	95.2	174.7	151.3	350.0		4.6	3.8	4.7	19.4	4.5	28.8	House mouse BU757735.1
44.2	350.0	350.0	167.9		4.8	6.4	5.6	4.4	6.8	8.8	16.0	House mouse BY775223.1
350.0	138.6	203.4		7.2	14.7	4.5	11.2	4.8	4.8	5.4	5.4	Pig AJ687535
350.0	209.4		5.1	5.2	4.3	4.4	9.7	3.6	5.5	84.9	1.7	Pig AJ94061
350.0		4.8	8.6	8.4	32.6	3.7	2.9	2.7	80.0	3.4	57.6	Norway rat
	3.4	5.0	4.8	52.0	3.2	9.0	4.1	3.2	2.5	4.3	12.8	Sheep

GH has more than 400 actions that are mediated by the GHR, which is widely expressed in nearly all body tissues [44,45]. *GHR* is highly expressed in liver and muscle tissues [15,16], and *0.7-kb GHR* is highly expressed in liver, skeletal muscle, and adipose tissues of dwarf chicken [18]. The current study indicated that *GHR-AS-EST* regulates GHR RNA and protein expression, as well as the signalling transduction from GH to GHR and GHR to downstream JAK/STAT, and JAK/SOCS signaling via GHBP in LMH cells. Considering the biological function of *GHR* in chicken muscle development and fat deposition, *GHR-AS-EST* can be considered as a candidate regulatory element for muscle development, fat deposition, and fat metabolism in chickens. Further exploration of the underlying mechanism of *GHR-AS-EST* in chicken muscle development and fat deposition will be of interest. It will be very important to assess whether

GHR-AS-EST-encoded protein exists *in vivo*. Both GH and IGF1 are involved in somatotropic axis (GH-GHR-IGF1). IGF1 is a very potent growth factor that stimulates growth in all cell types playing a critical role in pre- and postnatal growth [34]. Therefore, further exploration of changes in GH and IGF1 proteins caused by *GHR-AS-EST* might provide insights into the biological significance of *GHR-AS-EST* and details on its regulatory mechanism.

NATs are capable of controlling the epigenetic status of the promoter of their host genes [7,35,46]. Given that CpG sites of the *GHR* V1 promoter are more highly methylated in normal than dwarf WRR chicken livers [16] and that *GHR-AS-EST* is a GC-rich NAT located only 29 bp from the *GHR* V1 promoter, *GHR-AS-EST* might have a differential regulatory function in *GHR* V1 methylation between normal and dwarf WRR chickens. The chicken *GHR* gene produces different sense transcripts as a result of alternative usage of different 5′UTRs and functional polyadenylation signals [16,18–20]. Interestingly, our study identified two new *GHR* sense transcripts that have different 3′ UTRs, and contain different 5′UTRs of which differ from that of *GHR* mRNA. Hence, in future, we plan to investigate the potential function of *GHR-AS-EST* in regulating the *GHR* V1 promoter methylation level and in alternative splicing involving the 5′ UTR and polyadenylation signal of *GHR* sense transcripts.

Although several NATs are highly conserved in mammals [39,47], many NATs lack strong sequence conservation because their evolution does not involve the modification of corresponding protein-coding regions [48]. Interestingly, such weak evolutionary constraints not only allow the rapid generation of lncRNAs, but also contribute to rapid sequence evolution [49]. Rapid evolution of antisense lncRNAs enables rapid responses to and recovery from stimuli in organisms [48]. Our data revealed that chicken *GHR-AS-EST* exhibits low sequence conservation, and could not be found in other vertebrates included in the NCBI UniGene database. This may indicate low abundance or even total absence of *GHR-AS-EAT* in other species. Therefore, we infer that *GHR-AS-EST* is a species-specific antisense RNA.

In summary, we identified a novel chicken NAT, *GHR-AS-EST*, which shows very low sequence similarity with sequences in different other species, but strongly compliments its host gene, *GHR*, a primary regulator of muscle development and fat deposition. *GHR-AS-EST* might encode a ~ 17-kDa protein and regulates GHR RNA and protein expression via regulating the transcriptional activity of the *GHR* V1 promoter and forming an RNA duplex with GHBP. Although we evaluated the expression and function of *GHR-AS-EST* only in liver and muscle tissues of normal chicken, not sex-linked dwarf chickens, we carefully suggest that the differential fat deposition in these chicken lines might be affected by *GHR-AS-EST*. We believe that the discovery of *GHR-AS-EST* will aid further exploration into the molecular mechanisms of muscle development and fat deposition in chickens.

Materials and methods

Ethics statement

All animal procedures were authorized by the Animal Care Committee of South China Agricultural University (Guangzhou, China). Animals involved in the present study were humanely sacrificed and every attempt was made to minimize their suffering.

Animals and tissue collection

Six 16-day-old female normal embryonic WRR chickens bought from the Chicken Breeding Farm of South China Agricultural University (Guangzhou, China) were used. The following tissues were collected: cerebrum, cerebellum, hypothalamus, heart, liver, spleen, lung, kidney, breast muscle, leg muscle, glandular stomach, and gizzard. Tissue samples were immediately homogenized in liquid nitrogen.

RNA extraction and cloning of chicken GHR-AS

Total RNA was extracted from the chicken liver tissues using the TRIzol reagent (Invitrogen, Carlsbad, CA, USA). RNA integrity was assessed by agarose electrophoresis. RACE of chicken GHR-AS-EST was conducted using a RACE kit (Clontech, Japan) per the manufacturer's instruction, followed by nested PCRs of the cDNA copies. The PCR products were cloned and sequenced in the forward and reverse directions. All RACE primers are listed in Table S1.

Northern blotting

Northern blotting to evaluate *GHR-AS-EST* RNA expression in the chicken liver was conducted as described previously [16], with some modifications. RNA probe was designed to minimize non-specific hybridization through BLAST searches (http://blast.ncbi.nlm.nih.gov/). The selected 444-nt probe sequence for the detection of *GHR-AS-EST* (Table 2) was synthesized and labelled with biotin by Sangon Biotech Company (Shanghai, China).

Strand-specific RT-PCR

Total RNA was extracted using TRIzol (TaKaRa, Otsu, Japan) according to the manufacturer's instructions, and treated with gDNA Eraser (TaKaRa) at 42°C for 5 min. One microgram of RNA was reverse-transcribed into cDNA utilizing RT reagent Kit (TaKaRa) in 20-μL reactions at 50°C for 15 min, 85°C for 5 s. The reverse primer of GHR-AS-EST (5 pmol) was used as the RT primer. PCRs were carried out in 20-μL reactions including 5 μL strand-specific cDNA, 10 μL 2 × Taq PCR MasterMix (Tiangen, Beijing, China), and 0.5 μM forward and

Table 2. The single strand biotin-labelled probe, used for Northern blot to detect chicken *GHR-AS-EST*.

Application	Probe sequence (5′ to 3′, 444 bp)
GHR-AS-EST detection	actccttccattgggtctcattaacttatttgtactgcaattcatactccagagtaatccatcctttctgaacatctgctgttggtggtggatcccatcgtacttgaatatccccatggatc ccagtttgactagtatttagcagagtccagttaaggtgcacaggggatcaggtagtactatttcatcaacactgaaacacttttcgtcaaatacttcatctttattggcaagcttaac acaatatggtatccaaatcgaggtgtaggatgtgttgaagtaacagctattttctcctgcagtgatataatccggacattctttccagtcttcatcactccttttcatatacaacagttgt attgttcctgaagtagtgaggtttccatcagtccaataacacgaaaatgtctccagctcaggtgacctgcacttgctgattt

reverse primer. Thermal cycles were as follows: 94°C for 3 min, 35 cycles of 94°C for 30 s, 60°C for 30 s, and 72°C for 1 min, and finally, 72°C for 5 min.

Construction of expression plasmids

The sequences of *GHR-AS-EST* and the 0.7-kb *GHR* transcript were amplified by PCR, cleaved, and ligated into corresponding sites of pcDNA 3.1 to construct pc3.1-GHR-AS-EST and pc3.1-0.7-kb GHR. *GHR* V1 and ASP luciferase reporters constructs were generated by cloning the corresponding regions into the pGL3-basic vector by PCR. For qualitative analyses of the *GHR* V1 and ASP promoters, GFP luciferase reporters pV1-EGFP and pASP-EGFP were constructed by cloning the corresponding V1 and ASP regions into the pEGFP-N1 vector to substitute its CMV region, by PCR. The negative control vector pLinker-EGFP (without CMV region of pEGFP-N1) was constructed using deletion Ω-PCR as reported elsewhere [27]. To construct the Flag-tag expression plasmids, GH-CDS, GHR-FL-CDS, GHBP, 0.7-kb GHR and GHR-AS-EST were amplified by PCR from chicken liver cDNA. The PCR products were cleaved and ligated into the corresponding sites of pCMV-C-Flag (Beyotime Biotechnology, Guangzhou, China). To construct other tagged expression plasmids, cDNAs encoding full-length chicken GH, GHR-FL-CDS, GHBP, 0.7-kb GHR, and GHR-AS-EST, with their signal peptides if present, were separately amplified by PCR. The PCR products were inserted into the vector of pCMV-C-CFP, pCMV-C-EGFP, pCMV-C-YFP, pCMV-C-BFP, and/or pCMV-C-DsRed (Beyotime), producing X_Y constructs (X represents GH, GHR, GHBP, 0.7-kb GHR, or GHR-AS-EST, Y represents CFP, EGFP, YFP, BFP, or DsRed). Primers used in these experiments are listed in Table S1.

Cell culture and transfection

The chicken LMH cell line was a gift from the Harbin Veterinary Research Institute, Chinese Academy of Agricultural Science (Heilongjiang, China). Cells were cultured in high-glucose Dulbecco's modified Eagle's medium (Gibco, Grand Island, NY, USA) containing 10% fetal bovine serum (Invitrogen), penicillin (100 IU/mL), and streptomycin (100 μg/mL) (Invitrogen). Chicken primary myoblasts were isolated from 11-day-old chicken embryos and were cultured as described elsewhere [50]. All cells were maintained at 37°C in 5% CO_2.

For GHR-AS-EST overexpression and knockdown assays, cells were seeded in 12- or 24-well plates. When the cells reached 60–70% confluence, they were transfected with pc3.1-GHR-AS-EST or empty pcDNA3.1, and siRNA oligonucleotides or negative control (si-NC: GenePharma, Suzhou, China) (Table 3), using Lipofectamine 3000 (Invitrogen), following the manufacturer's instructions. Forty-eight hours post-transfection, the cells were harvested and stored at −80° C for further analysis.

Rt-qPCR

Total RNA was reverse-transcribed to cDNA using Oligo-dT and random 6mers, and the PrimeScript RT Master Mix kit (TaKaRa, Otsu, Japan) per the manufacturer's instructions. qPCRs were run in triplicate on a Bio-Rad CFX96 Real-Time Detection system (Bio-Rad, Hercules, California, USA) using the SYBR Premix ExTaq kit (TaKaRa, Otsu, Japan). Primers used for RT-qPCR were designed by Primer5 software and sequences are shown in Table S1. Relative target gene expression levels were calculated using the $2^{-\Delta\Delta Ct}$ method and were normalized to chicken *β-actin* expression.

Reporter assays

For luciferase reporter assays, cells were seeded in triplicate into 24-well plates at 2.5×10^5 cells/well and co-transfected with the indicated reporter plasmid, pRL-TK vector (Promega) encoding Renilla luciferase, empty pcDNA 3.1, or pc3.1-GHR-AS-EST overexpression vector using Lipofectamine 3000. At 48 h after transfection, cells were lysed with passive lysis buffer, and luciferase activity was measured using the Dual-Luciferase® Assay System (Promega) per the manufacturer's protocols. For GFP detection, LMH cells were inoculated into 24-wells plates at 2.5×10^5 cells/well. The cells were transfected with pV1-EGFP and pASP-EGFP using Lipofectamine 3000. At 48 h after transfection, fluorescence was observed under a Leica DMi8 system (Leica, Germany).

Endogenous ribonuclease protection assay

To detect the RNA duplex formed by *GHR* sense and antisense RNAs, endogenous ribonuclease protection assay was performed as previously described [16,31,40], with minor modifications, using total RNA from chicken liver and leg muscle tissues, LMH cells and primary myoblasts. To remove genomic DNA and single-strand RNA, the total RNA was treated with DNase I (TaKaRa, Otsu, Japan) at 37°C for 30 min and then digested with RNase A (20 ng/μL; TaKaRa) 37°C for 1 h. Following the RNase A protection assay, we used RT-PCR to detect duplex formation. Five sets of primers were designed for PCR: a first set was targeted to the *GHR-AS-EST* full-length region of the *GHR* sense and antisense transcripts, and the other sets were targeted to different overlapping regions of these transcripts (Table S1). PCRs were run in 35 cycles using 25-μL reactions and 2 × Taq PCR Master Mix

Table 3. siRNA targeting chicken *GHR-AS-EST*.

	Sequence (5′ to 3′)	
si-RNA Name	Sense	Antisense
si-GHR-AS-EST	CCUUCCAUUGGGUCUCAUUTT	AAUGAGACCCAAUGGAAGGTT
si-Negative control (si-NC)	UUCUCCGAACGUGUCACGUTT	ACGUGACACGUUCGGAGAATT

(Tiangen). Products were checked by 2% agarose gel electrophoresis.

RNA stability assay

RNA stability was assayed as described previously [25]. Chicken primary myoblasts transfected with 1 μg of pc3.1-GHR-AS-EST or empty pcDNA3.1 were seeded into 12-well plates. After 48 h, the cells were treated with 2 μg/mL actinomycin D (Sigma-Aldrich, St. Louis, MO, USA) to inhibit transcription and harvested 0, 2, 4 h, 6 h, 8 h, and 10 h later. Total RNA was extracted for RT-PCR and residual mRNAs were detected by RT-qPCR. Three independent samples were detected for each data point, *GAPDH* was used as internal control gene because its half-life is more than 30 h [25].

Western blotting

Cellular protein was extracted using lysis buffer (0.5% Triton X-100, 150 mM NaCl, 50 mM Tris–HCl, 2 mM EDTA, and 1 mM PMSF). The proteins were separated by 8% SDS-PAGE and transferred onto a Hybond membrane (Amersham). Membranes were blocked with 5% milk in phosphate-buffered saline (PBS) for 1 h and then incubated with the primary antibodies anti-Flag (1:1000) and β-tubulin (1:1000) (Beyontime) for 2 h. Then, the membranes were probed with antibody anti-mouse IgG (Beyontime). Target proteins were detected using an enhanced chemiluminescence detection system (Pierce, Rockford, IL, USA).

Fluorescence co-localization assay

To generate cells co-expressing GH_{CFP}, GHR_{EGFP}, $GHBP_{YFP}$, 0.7-kb GHR_{BFP}, and GHR-AS-EST_{DsRed}, LMH cells were co-transfected with 0.5 μg of each of the corresponding plasmids using Lipofectamine 3000. After 48 h of culture, the cells were washed with cold PBS and fixed in cold 4% formaldehyde in PBS for 4 min at room temperature. Images were captured under a confocal laser scanning microscope (Leica). Filters used for observing GH_{CFP} allowed excitation at 458 nm and emission at 465–495; for GHR_{EGFP}, allowed excitation at 488 nm and emission at 495–525 nm; for $GHBP_{YFP}$, allowed excitation at 513 nm and emission at 518–548 nm; for 0.7 kb GHR_{BFP}, allowed excitation at 382 nm and emission at 435–-465 nm; and for GHR-AS-EST_{DsRed}, allowed excitation at 558 nm and emission at 570–600 nm.

FRET measurements

To generate co-expressing GH_{BFP}/$GHBP_{DsRed}$, GH_{BFP}/0.7-kb GHR_{DsRed}, GH_{BFP}/GHR-AS-EST_{DsRed}, $GHBP_{BFP}$/0.7-kb GHR_{DsRed}, $GHBP_{BFP}$/GHR-AS-EST_{DsRed}, and GHR-AS-EST_{BFP}/0.7-kb GHR_{DsRed} cells, chicken primary myoblasts were co-transfected with 2 μg of each group of these six constructs using Lipofectamine 3000. After 48 h of culture, the cells were image under the Leica confocal laser scanning microscope as described above. Filters used for observing GH_{BFP}, $GHBP_{BFP}$, or GHR-AS-ESR_{BFP} allowed excitation at 382 nm and emission at 435–465 nm; for $GHBP_{DsRed}$, 0.7-kb GHR_{DsRed}, or GHR-AS-EST_{DsRed} excitation at 558 nm and emission at 570–600 nm was used; for FRET of these six constructs, excitation was at 382 nm and emission at 570–600 nm.

Cell proliferation assay

Cells transfected with pc3.1-GHR-AS-EST or si-GHR-AS-EST and control cells were harvested after 72 h of culture, washed with cold PBS, and fixed in 1 mL of cold 70% ethanol. After overnight incubation at – 20°C in ethanol, cells were washed in PBS and suspended in 500 mL propidine iodide (PI) solution for 30 min before flow cytometry. Populations in G1, S, and G2 phases were measured by flow cytometry (Beckman, CA, USA), and the data were analyzed using Multicycle-DNA Cell Cycle Analysis Software. Measurements were conducted in quadruplicate. Additionally, transfected cells were seeded in 96-well flat-bottom plates at 2×10^3 cells/well in 200 μL of medium and were cultured for 12 h, 24 h, 36 h, and 48 h. The Cell Counting Kit-8 (CCK-8) (Transgen, Guangzhou, China) was used per the manufacturer's instructions to assay proliferation. DNA synthesis in proliferating cells was determined by the EdU assay, using the Cell-Light^{TM} EdU Appolo567 In Vitro Kit (Ribobio, Shanghai, China) following the manufacturer's protocol. Treated cells were observed under the Leica fluorescence microscope. Experiments were repeated at least three times in duplicate.

Oil Red O staining

To analyze the effect of GHR-AS-EST on fat deposition in the chicken liver, LMH cells transfected with si-GHR-AS-EST or pc3.1-GHR-AS-EST and control cells were stained with Oil Red O. After 48 h of transfection, cells were washed twice with cold PBS, fixed with 10% paraformaldehyde for 30 min, stained with Oil Red O at room temperature for 15 min, and observed under a light microscope (Nikon, Tokyo, Japan).

Statistical analysis

All experimental data are as means ± SEMs of at least three independent experiments. SPSS software was used for statistical analysis. Student's t-test was used for individual comparisons. Difference between groups was considered statistically significant if $p < 0.05$.

GHR-AS-EST sequence similarity analysis

The whole sequence of chicken *GHR-AS-EST* was determined in this study, and *GHR-AS* sequences for nine other species (human: AA398260.1, cattle: CK848828.1, dog: CX009677.1, house mouse: BU757735 and BY775223.1, sheep: S78251, Japanese medaka: DC276396, pig: AJ940615 and AJ687535, African clawed frog: BI441774, Norway rat: AW533500) were downloaded from the NCBI UniGene database. The DNAStar-EdiSeq tool was used to translate the potential coding regions of each *GHR-AS* sequence. Similarity among either nucleotide or proteins sequences was assessed using

Clustal Omega (https://www.ebi.ac.uk/Tools/msa/) [51,52]. Nnucleotide similarity between two species was tested by pairwise searches using BLAST2N [53], and pair distances were analyzed using MEGA6.0 software [54]. Similarity of potential coding regions was assessed using BLAST Multiple Alignment Tool [55] and that between two species was tested using BLAST2P with a similarity E-value <0.001 [53].

Acknowledgments

We thank Prof. Yunfeng Wang and Yan Zhao (Harbin Veterinary Research Institute, Chinese Academy of Agricultural Science, Heilongjiang, China) for giving us LMH cells.

Disclosure of potential conflicts of interest

No potential conflicts of interest were disclosed.

Funding

This work was funded by the China Agriculture Research System (CARS-41-G03), the National Natural Science Foundation of China (31672412), and the Graduate Student Overseas Study Program from South China Agricultural University (Grant No. 2017LHPY016).

Author Contributions

SL wrote the paper, analyzed data and designed the figures; SL, WL, QN and XZ conceived and designed this study; SL, ZZ, and TX performed experiments; both BH and ZR helped a lot during these experiments; LZ, CL, and CL put forward many precious suggestions to improve the quality of this draft; X.Z. gave a lot of valuable opinions for modification and finalized the manuscript.

ORCID

Congjun Li http://orcid.org/0000-0003-1389-9820

References

[1] Watanabe K, Kamiya D, Nishiyama A, et al. Directed differentiation of telencephalic precursors from embryonic stem cells. Nat Neurosci. 2005;8(3):288–296.
[2] Faghihi MA, Wahlestedt C. Regulatory roles of natural antisense transcripts. Nat Rev Mol Cell Biol. 2009;10(9):637–643.
[3] Yuan C, Wang J, Harrison AP, et al. Genome-wide view of natural antisense transcripts in arabidopsis thaliana. Dna Res. 2015;22(3):233–243.
[4] Lapidot M, Pilpel Y. Genome-wide natural antisense transcription: coupling its regulation to its different regulatory mechanisms. Embo Rep. 2006;7(12):1216–1222.
[5] Lin S, Zhang L, Luo W, et al. Characteristics of antisense transcript promoters and the regulation of their activity. Int J Mol Sci. 2016;17(1):9.
[6] Luo S, Lu JY, Liu L, et al. Divergent lncRNAs regulate gene expression and lineage differentiation in pluripotent cells. Cell Stem Cell. 2016;18(5):637–652.
[7] Cui I, Cui H. Antisense RNAs and epigenetic regulation. Epigenomics. 2010;2(1):139–150.
[8] Sun Y, Li D, Zhang R, et al. Strategies to identify natural antisense transcripts. Biochimie. 2017;132:131–151.
[9] Kashi K, Henderson L, Bonetti A, et al. Discovery and functional analysis of lncRNAs: methodologies to investigate an uncharacterized transcriptome. Biochim Biophys Acta. 2016;1859(1):3–15.
[10] Muret K, Klopp C, Wucher V, et al. Long noncoding RNA repertoire in chicken liver and adipose tissue. Genet Sel Evol. 2017;49(1):6.
[11] Weikard R, Demasius W, Kuehn C. Mining long noncoding RNA in livestock. Anim Genet. 2017;48(1):3–18.
[12] Carrieri C, Cimatti L, Biagioli M, et al. Long non-coding antisense RNA controls Uchl1 translation through an embedded SINEB2 repeat. Nature. 2012;491(7424):454–457.
[13] Zinad HS, Natasya I, Werner A. Natural antisense transcripts at the interface between host genome and mobile genetic elements. Front Microbiol. 2017;8. DOI:10.3389/fmicb.2017.02292.
[14] Waters MJ, Brooks AJ. Growth hormone receptor: structure function relationships. Horm Res Paediatr. 2011;76(s1):12–16.
[15] Lin S, Li H, Mu H, et al. Let-7b regulates the expression of the growth hormone receptor gene in deletion-type dwarf chickens. Bmc Genomics. 2012;13:306.
[16] Zhang L, Lin S, An L, et al. Chicken GHR natural antisense transcript regulates GHR mRNA in LMH cells. Oncotarget. 2016;7(45):73607.
[17] Lin S, Li C, Li C, et al. Growth hormone receptor mutations related to individual dwarfism. Int J Mol Sci. 2018;19(5):1433.
[18] Oldham ER, Bingham B, Baumbach WR. A functional polyadenylation signal is embedded in the coding region of chicken growth hormone receptor RNA. Mol Endocrinol. 1993;7(11):1379–1390.
[19] Huang N, Cogburn LA, Agarwal SK, et al. Overexpression of a truncated growth hormone receptor in the sex-linked dwarf chicken: evidence for a splice mutation. Mol Endocrinol. 1993;7(11):1391–1398.
[20] Lau JS, Yip CW, Law KM, et al. Cloning and characterization of chicken growth hormone binding protein (cGHBP). Domest Anim Endocrinol. 2007;33(1):107–121.
[21] Burnside J, Liou SS, Zhong C, et al. Abnormal growth hormone receptor gene expression in the sex-linked dwarf chicken. Gen Comp Endocrinol. 1992;88(1):20–28.
[22] Figueiredo MA, Mareco EA, Silva MD, et al. Muscle-specific growth hormone receptor (GHR) overexpression induces hyperplasia but not hypertrophy in transgenic zebrafish. Transgenic Res. 2012;21(3):457–469.
[23] Katayama S, Tomaru Y, Kasukawa T, et al. Antisense transcription in the mammalian transcriptome. Science. 2005;309(5740):1564–1566.
[24] Zhang L, Li Y, Xie X, et al. A systematic analysis on mRNA and microRNA expression in runting and stunting chickens. Plos One. 2015;10(5):e127342.
[25] Wang Y, Pang W, Wei N, et al. Identification, stability and expression of Sirt1 antisense long non-coding RNA. Gene. 2014;539(1):117–124.
[26] Cai B, Li Z, Ma M, et al. LncRNA-Six1 encodes a micropeptide to activate Six1 in Cis and is involved in cell proliferation and muscle growth. Front Physiol. 2017;8. DOI:10.3389/fphys.2017.00230.
[27] Lin S, Luo W, Jiang M, et al. Chicken CCDC152 shares an NFYB-regulated bidirectional promoter with a growth hormone receptor antisense transcript and inhibits cells proliferation and migration. Oncotarget. 2017;8(48). DOI:10.18632/oncotarget.21091
[28] Lee JT, Davidow LS, Warshawsky D. Tsix, a gene antisense to Xist at the X-inactivation centre. Nat Genet. 1999;21(4):400–404.
[29] Yu W, Gius D, Onyango P, et al. Epigenetic silencing of tumour suppressor gene p15 by its antisense RNA. Nature. 2008;451(7175):202–206.
[30] Sarkar MK, Gayen S, Kumar S, et al. An Xist-activating antisense RNA required for X-chromosome inactivation. Nat Commun. 2015;6(1). DOI:10.1038/ncomms9564
[31] Liu P, Jin L, Zhao L, et al. Identification of a novel antisense long non-coding RNA PLA2G16 -AS that regulates the expression of PLA2G16 in pigs. Gene. 2018;671:78–84.
[32] Ling K, Brautigan PJ, Moore S, et al. Derivation of an endogenous small RNA from double-stranded Sox4 sense and natural antisense transcripts in the mouse brain. Genomics. 2016;107(2–3):88–99.

[33] Pereira Fernandes D, Bitar M, Jacobs F, et al. Long non-coding RNAs in neuronal aging. Noncoding RNA. 2018;4(2):12.
[34] Wójcik M, Krawczyńska A, Antushevich H, et al. Post-receptor inhibitors of the GHR-JAK2-STAT pathway in the growth hormone signal transduction. Int J Mol Sci. 2018;19(7):1843.
[35] Li Q, Su Z, Xu X, et al. AS1DHRS4, a head-to-head natural antisense transcript, silences the DHRS4 gene cluster in cis and trans. Proc Natl Acad Sci USA. 2012;109(35):14110–14115.
[36] Halley P, Kadakkuzha BM, Faghihi MA, et al. Regulation of the apolipoprotein gene cluster by a long noncoding RNA. Cell Rep. 2014;6(1):222–230.
[37] Goyal A, Fiškin E, Gutschner T, et al. A cautionary tale of sense-antisense gene pairs: independent regulation despite inverse correlation of expression. Nucleic Acids Res. 2017;45 (21):12496–12508.
[38] Yamanaka Y, Faghihi MA, Magistri M, et al. Antisense RNA controls LRP1 sense transcript expression through interaction with a chromatin-associated protein, HMGB2. Cell Rep. 2015;11 (6):967–976.
[39] Scheele C, Petrovic N, Faghihi MA, et al. The human PINK1 locus is regulated in vivo by a non-coding natural antisense RNA during modulation of mitochondrial function. Bmc Genomics. 2007;8:74.
[40] Li K, Ramchandran R. Natural antisense transcript: a concomitant engagement with protein-coding transcript. Oncotarget. 2010;1 (6):447.
[41] Quinteiro C, Castro-Feijoo L, Loidi L, et al. Novel mutation involving the translation initiation codon of the growth hormone receptor gene (GHR) in a patient with Laron syndrome. J Pediatr Endocrinol Metab. 2002;15(7):1041–1045.
[42] Rosenbloom AL. Physiology and disorders of the growth hormone receptor (GHR) and GH-GHR signal transduction. Endocrine. 2000;12(2):107–119.
[43] Derr MA, Aisenberg J, Fang P, et al. The growth hormone receptor (GHR) c.899dupC mutation functions as a dominant negative: insights into the pathophysiology of intracellular GHR defects. J Clin Endocrinol Metab. 2011;96(11):E1896–904.
[44] Waters MJ, Hoang HN, Fairlie DP, et al. New insights into growth hormone action. J Mol Endocrinol. 2006;36(1):1–07.
[45] Hainan L, Huilin L, Khan M, et al. The basic route of the nuclear translocation porcine growth hormone (GH)-growth hormone receptor (GHR) complex (pGH/GHR) in porcine hepatocytes. Gen Comp Endocrinol. 2018;266:101–109.
[46] Xi Q, Gao N, Zhang X, et al. A natural antisense transcript regulates acetylcholinesterase gene expression via epigenetic modification in Hepatocellular Carcinoma. Int J Biochem Cell Biol. 2014;55:242–251.
[47] Ling MH, Ban Y, Wen H, et al. Conserved expression of natural antisense transcripts in mammals. Bmc Genomics. 2013;14:243.
[48] Pelechano V, Steinmetz LM. Gene regulation by antisense transcription. Nat Rev Genet. 2013;14(12):880–893.
[49] Pang KC, Frith , MC, Mattick JS. Rapid evolution of noncoding RNAs: lack of conservation does not mean lack of function. Trends Genet. 2006;22(1):1–05.
[50] Li G, Luo W, Abdalla BA, et al. miRNA-223 upregulated by MYOD inhibits myoblast proliferation by repressing IGF2 and facilitates myoblast differentiation by inhibiting ZEB1. Cell Death Dis. 2017;8(10):e3094.
[51] Troshin PV, Procter JB, Sherstnev A, et al. JABAWS 2.2 distributed web services for bioinformatics: protein disorder, conservation and RNA secondary structure. Bioinformatics. 2018;34 (11):1939–1940.
[52] Sievers F, Higgins DG. Clustal omega for making accurate alignments of many protein sequences. Protein Sci. 2018;27 (1):135–145.
[53] Yuan J, Bush B, Elbrecht A, et al. Enhanced homology searching through genome reading frame predetermination. Bioinformatics. 2004;20(9):1416–1427.
[54] Tamura K, Stecher G, Peterson D, et al. MEGA6: molecular evolutionary genetics analysis version 6.0. Mol Biol Evol. 2013;30(12):2725–2729.
[55] McGinnis S, Madden TL. BLAST: at the core of a powerful and diverse set of sequence analysis tools. Nucleic Acids Res. 2004;32 (WebServer):W20–25.